understory canopy varied from 85% in *C. flexuosus* communities, to 70% in *A. setacea* communities, and 60% in mixture communities.

Experimental design

The experimental design was a 2×3 factorial experiment with two burning treatments (burned and unburned) and three grazing treatments (natural levels of grazing, ungrazed and experimentally clipped). All experimental plots were $4\,m \times 4\,m$, located within an area of $\sim 1\,km^2$, subject to similar climate conditions and potentially shared a common species pool. Overall, there were nine replicates for each unburned treatment and 18 for treatment combinations involving burning (three and six in each of three community types, respectively). Plots not experimentally manipulated (unburned, naturally grazed treatments) were excluded from the analysis. At each sampling session, species richness and cover was enumerated in eight and four $1\text{-}m^2$ sub-plots, respectively, using a stratified sampling scheme. Species cover in sub-plots was estimated using a $1\,m \times 1\,m$ grid frame subdivided into 100 units of $0.01\,m^2$ each. Data reported here are for one year following experimental manipulations, and are therefore devoid of any seasonal biases. Where necessary, they were transformed to fit the assumptions of normality.

Indices

$R_c = \Sigma$ minimum (p_{ii}, p_{of}), where p_{ii} and p_{if} represent the relative cover of the *i*th species in pre-disturbance and 1 year post-disturbance plots, respectively[22]. $R_{st} = N_{com}/N_{tot}$, where N_{tot} represents the total number of distinct species recorded in pre-disturbance and 1 year post-disturbance plots, and N_{com} represents the number of species common to pre-disturbance and 1 year post-disturbance plots. Diversity was calculated using the Shannon–Weiner index[29] as $H' = \Sigma\, p_i \ln(p_i)$, where p_i represents the proportional contribution of the *i*th species to the canopy. Proneness of communities to different disturbance combinations was calculated as $P_{bg} = P_b + P_g$, where the subscripts b and g represent the specific burning and grazing treatments. Proneness to burning was determined on the basis of the cover of *C. flexuosus* present initially in the plot (P_c). Burned treatments were assigned the value P_c whereas unburned treatments were assigned a value of $(1 - P_c)$ for this index. We believe that this is a valid index because *C. flexuosus* individuals are characteristic of the fire-prone environments, and also promote fires because of the extent of litter and standing dead biomass they produce. For the grazing treatments, grazed and clipped plots were assigned the value P_g and ungrazed plots $(1 - P_g)$, where P_g represents the fraction of species initially grazed in plots.

1. Wilson, E. O. *The Diversity of Life* (Norton, New York, 1992).
2. Steadman, D. W. in *Biodiversity II* (eds Reaka-Kudla, M. L., Wilson, D. E. & Wilson, E. O.) 139–162 (Joseph Henry, Washington DC, 1997).
3. Russell, G. J., Brooks, T. M., McKinney, M. M. & Anderson, C. G. Present and future taxonomic selectivity in bird and mammal extinctions. *Conservation Biol.* **12**, 1365–1376 (1998).
4. Schulze, E. D. & Mooney, H. A. (eds) *Biodiversity and Ecosystem Function* (Springer, Berlin, 1993).
5. Hurd, L. E., Mellinger, M. V., Wolf, L. L. & McNaughton, S. J. Stability and diversity at three trophic levels in terrestrial ecosystems. *Science* **173**, 1134–1136 (1971).
6. McNaughton, S. J. Diversity and stability of ecological communities: a comment on the role of empiricism in ecology. *Am. Nat.* **111**, 515–525 (1977).
7. McNaughton, S. J. in *Biodiversity and Ecosystem Function* (eds Schulze, E. D. & Mooney, H. A.) 361–383 (Springer, Berlin, 1993).
8. Tilman, D. & Downing, J. A. Biodiversity and stability in grasslands. *Nature* **367**, 363–365 (1994).
9. Naeem, S., Thompson, L. J., Lawler, S. P., Lawton, J. H. & Woodfin, R. M. Declining diversity can alter the performance of ecosystems. *Nature* **368**, 734–737 (1994).
10. Naeem, S., Thompson, L. J., Lawler, S. P., Lawton, J. H. & Woodfin, R. M. Empirical evidence that declining diversity can alter the performance of ecosystems. *Phil. Trans. R. Soc. Lond. B.* **347**, 249–262 (1995).
11. Tilman, D., Wedin, D. & Knops, J. Productivity and sustainability influenced by biodiversity in grassland ecosystems. *Nature* **379**, 718–720 (1996).
12. Naeem, S., Hakansson, K., Lawton, J. H., Crawley, M. J. & Thompson, L. J. Biodiversity and productivity in a model assemblage of plant species. *Oikos* **76**, 259–264 (1996).
13. Grady-Steed, J., Harris, P. M. & Morin, P. J. Biodiversity regulates ecosystem predictability. *Nature* **390**, 162–165 (1997).
14. Naeem, S. & Li, S. Biodiversity enhances ecosystem reliability. *Nature* **390**, 507–509 (1997).
15. Tilman, D. *et al.* The influence of functional diversity on ecosystem processes. *Science* **277**, 1300–1302 (1997).
16. Hooper, D. U. & Vitousek, P. M. The effect of plant composition and diversity on ecosystem processes. *Science* **277**, 1302–1305 (1997).
17. Hooper, D. U. & Vitousek, P. M. Effects of plant composition and diversity on nutrient cycling. *Ecol. Monogr.* **68**, 121–149 (1998).
18. MacGillivray, C. W. *et al.* Testing predictions of the resistance and resilience of vegetation subjected to extreme events. *Functional Ecol.* **9**, 640–649 (1995).
19. Huston, M. A. Hidden treatments in ecological experiments: re-evaluating the ecosystem function of biodiversity. *Oecologia* **110**, 449–460 (1997).
20. Grime, J. P. Biodiversity and ecosystem function: the debate deepens. *Science* **277**, 1260–1261 (1997).
21. Wardle, D. A. A more reliable design for biodiversity study? *Nature* **394**, 30 (1998).
22. Frank, D. A. & McNaughton, S. J. Stability increases with diversity in plant communities: empirical evidence from the 1988 Yellowstone drought. *Oikos* **62**, 360–362 (1991).
23. Doak, D. F. *et al.* The statistical inevitability of stability-diversity relations in community ecology. *Am. Nat.* **151**, 264–276 (1998).
24. Tilman, D., Lehman, C. L. & Bristow, C. E. Diversity-stability relationships: statistical inevitability or ecological consequence. *Am. Nat.* **151**, 277–282 (1998).
25. Ricklefs, R. E. Community diversity: relative roles of local and regional processes. *Science* **235**, 167–171 (1987).
26. Barbault, R. & Sastrapradja, S. in *Global Biodiversity Assessment* (ed. Heywood, V. H.) 193–274 (Cambridge Univ. Press, 1995).
27. Tilman, D. Biodiversity: population versus ecosystem stability. *Ecology* **77**, 350–363 (1996).
28. Pimm, S. L. *The Balance of Nature?* (Univ. Chicago Press, 1991).
29. MacArthur, R. H. Fluctuations of animal populations and a measure of community stability. *Ecology* **36**, 533–536 (1955).

···

Symmetry in locomotor central pattern generators and animal gaits

Martin Golubitsky*, Ian Stewart†, Pietro-Luciano Buono‡ & J. J. Collins§

* *Mathematics Department, University of Houston, Houston, Texas 77204-3476, USA*
† *Mathematics Institute, University of Warwick, Coventry CV4 7AL, UK*
‡ *Mathematics Institute, University of Warwick, Coventry CV4 7AL, UK*
§ *Department of Biomedical Engineering, Center for BioDynamics, Boston University, 44 Cummington Street, Boston, Massachusetts 02215, USA*

···

Animal locomotion is controlled, in part, by a central pattern generator (CPG), which is an intraspinal network of neurons capable of generating a rhythmic output[1–4]. The spatio-temporal symmetries of the quadrupedal gaits walk, trot and pace[5–8] lead to plausible assumptions about the symmetries of locomotor CPGs[9–11]. These assumptions imply that the CPG of a quadruped should consist of eight nominally identical subcircuits, arranged in an essentially unique matter. Here we apply analogous arguments to myriapod CPGs. Analyses based on symmetry applied to these networks lead to testable predictions, including a distinction between primary and secondary gaits, the existence of a new primary gait called 'jump', and the occurrence of half-integer wave numbers in myriapod gaits. For bipeds, our analysis also predicts two gaits with the out-of-phase symmetry of the walk and two gaits with the in-phase symmetry of the hop. We present data that support each of these predictions. This work suggests that symmetry can be used to infer a plausible class of CPG network architectures from observed patterns of animal gaits.

The architecture of CPGs is seldom observable *in vivo*. Aspects of CPG structure are therefore usually inferred from observable gait features such as the phase of the gait cycle at which a given limb hits the ground, and the 'duty factor'—the proportion of the gait cycle that a limb is in contact with the ground. It is usual to model CPGs as networks of nominally identical systems of differential equations, variously described[9–17] as 'units', 'oscillators' or 'cells'. We use the term 'cell'.

Here we discuss a schematic CPG network[10] (Fig. 1) that has twice as many cells as the animal has legs. For expository purpose we assume that cells 1, …, 2*n* determine the timing of leg movements, and refer to the remaining cells as 'hidden'.

The structure of the CPG network for a quadruped shown in Fig. 1b can be deduced from six assumptions: (1) the abstract CPG network is composed of identical cells, and the signal from each cell goes to one leg; (2) different gaits are generated by the same

network, and switching between gaits arises from changes in parameters (such as coupling strengths); (3) the locomotor CPG has the same architecture for all quadrupeds; (4) the network can generate the rhythms of walk, trot and pace; (5) trot and pace are dynamically independent, existing in different regions of parameter space; (6) the network generates only simple rhythmic patterns observed in quadrupedal locomotion.

The first assumption introduces symmetry into model CPGs[9–11,15] and accounts for the observed symmetries of many gaits[5–8]. Different CPGs could control the rhythms of each gait; but there would then have to be a controller that activates each CPG at the correct times, and there is no evidence for such controllers. It seems more likely that the second assumption is valid. Similarly, there is an evolutionary advantage in having a single architecture valid for all quadruped locomotor CPGs, thus justifying the third assumption.

As virtually all quadrupeds walk and either trot or pace, the network must produce these gaits, and so the fourth assumption seems appropriate. As camels pace but do not trot, and squirrels trot but do not pace, the fifth assumption must be valid. Finally, the sixth assumption is required in order to create the simplest CPG model.

We prove[18] that any CPG satisfying all six assumed conditions must consist of eight identical cells, whose interconnections have the same symmetry as Fig. 1b. There are two types of symmetry in the network: contralateral symmetry, that interchanges cells on the left with cells on the right; and ipsilateral symmetry, that cyclically and simultaneously permutes cells on both left and right.

There are two types of symmetries of a periodic solution: spatial symmetries, which fix the solution at each point in time; and spatio-temporal symmetries, which fix the solution only after a phase shift. For example, in a pace, interchanging fore and hind legs is a spatial symmetry, whereas interchanging right and left legs coupled with a half-period phase shift is a spatio-temporal symmetry.

Symmetries of differential equations force well-defined spatio-temporal relations (like half-period phase shifts) on periodic solutions[19]. A symmetry type of periodic solutions is called robust if small symmetric perturbations of the equations do not change the symmetries of the periodic solution. If no symmetries are present, then small perturbations of the equations are extremely likely to change the phase relations.

For coupled cell systems, we prove the following[18]. Let H be the subgroup of spatio-temporal symmetries and let $K \subset H$ be the subgroup of spatial symmetries; then the only robust types of periodic solutions of coupled cell systems are those for which the

quotient group H/K is cyclic. The most symmetric solutions are the ones for which the group H is the symmetry group of the network.
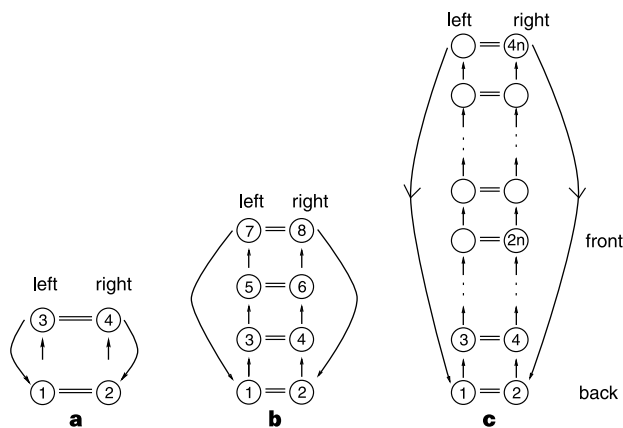
Table 1 lists the most symmetric rhythms; these correspond to standard quadrupedal gaits with the exception of the 'jump'. For concrete networks, the values of the coupling terms in the network dynamics determine which rhythms occur (refs 18, 20; P.-L. Buono, manuscript in preparation).

The eight-cell network in Fig. 1b is the only one that satisfies all six assumptions[10,18]. We sketch the argument. Walk implies that the network must have a four-cycle symmetry, and either trot or pace implies that the network must have a two-cycle symmetry. These statements follow from the first and fourth assumptions. The second assumption implies that the network must possess both of these symmetries.

The four-cycle symmetry implies that the number of cells is a multiple of four. If the network has four cells, then the two-cycle and four-cycle symmetries cannot commute and this forces trot and pace to be conjugate solutions, contradicting the fifth assumption. If the network has more than eight cells, then unnatural phase-shift symmetries would be allowed, negating the sixth assumption. Thus there are eight cells. In an eight-cell network, the fifth assumption implies that the four-cycle and two-cycle symmetries commute, and this leads to the network whose symmetry type is indicated in Fig. 1b. By analogy, the gaits of $2n$-legged animals require a network with the same symmetries as Fig. 1c.

Even though our model prescribes only the symmetries of the CPG, and not the differential equations, it still leads to several predictions:

Prediction 1. In our model, a gait is primary if the signal from each cell is identical up to phase shift. Secondary gaits are those where the signals to different legs are different waveforms. Our network produces six primary gaits[10] (see Table 1) and solutions that resemble gallops and canters (refs 10, 20; P.-L. Buono, manuscript

Table 1 Phase shifts for primary gaits in the eight-cell network

		Walk		Jump		Trot		Pace		Bound		Pronk	
LF	RF	$\pm\frac{3}{4}$	$\pm\frac{1}{4}$	$\frac{1}{2}$	$\frac{1}{2}$	$\frac{1}{2}$	0	0	$\frac{1}{2}$	$\frac{1}{2}$	$\frac{1}{2}$	0	0
LH	RH	$\pm\frac{1}{2}$	0	$\pm\frac{3}{4}$	$\pm\frac{3}{4}$	0	$\frac{1}{2}$	0	$\frac{1}{2}$	0	0	0	0
LF	RF	$\pm\frac{1}{4}$	$\pm\frac{3}{4}$	0	0	$\frac{1}{2}$	0	$\frac{1}{2}$	$\frac{1}{2}$	$\frac{1}{2}$	$\frac{1}{2}$	0	0
LH	RH	0	$\frac{1}{2}$	$\pm\frac{1}{4}$	$\pm\frac{1}{4}$	0	$\frac{1}{2}$	0	$\frac{1}{2}$	0	0	0	0

LF, left fore leg; RF, right fore leg; LH, left hind leg; RH, right hind leg.

Figure 1 Schematic central pattern generator (CPG) networks. **a**, Four-cell network for bipedal locomotor CPG; **b**, eight-cell network for quadrupeds; **c**, $4n$-cell network for $2n$-legged animals. Double lines indicate contralateral coupling; single lines indicate ipsilateral coupling. Direction of ipsilateral coupling is indicated by arrows; contralateral coupling is bidirectional.
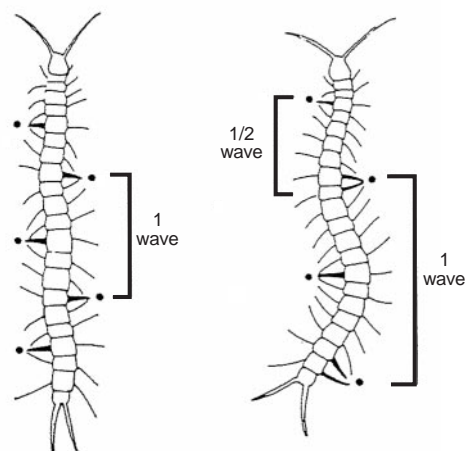
Figure 2 Half-integer wave numbers in myriapod gaits. Figure of Manton[25] from Alexander[5]. Thick lines indicate centipede legs in contact with the ground. Left centipede shows 3 waves. Right centipede shows 3/2 waves.

Table 2 Bipedal gaits for a four-cell CPG network

Slow hop		Fast hop		Walk		Run	
0	0	$\frac{1}{2}$	$\frac{1}{2}$	$\frac{1}{2}$	0	0	$\frac{1}{2}$
0	0	0	0	0	$\frac{1}{2}$	0	$\frac{1}{2}$

in preparation), which are secondary gaits. Experimentally observed variability from exact quarter-period and half-period phase shifts[21,22] can, in principle, be accounted for by analysing symmetry-broken secondary gaits. As the signals sent to fore legs in primary gaits are identical and in secondary gaits are unequal, the duty factors of the fore legs should be equal in primary gaits and unequal in secondary gaits. Indeed, the duty factors of fore legs of a walking horse are equal[8] and those of a galloping horse are different[23,24].

Prediction 2. Table 1 includes a non-standard primary gait, the jump, which can be described as 'fore feet hit ground, then hind feet hit ground, then three beats later fore feet hit ground'. We observed a gait with that pattern in a bucking bronco. (A figure showing four equal-time-interval frames, taken from a video provided by The Houston Livestock Show and Rodeo of the bareback bronco event on 24 February 1999, is available electronically at ftp://ftp.math.uh.edu/pub/laode/rodeo.) The timing of the footfalls is close to 0 and 1/4 of the period of this rhythmic motion. The primitive ricocheting jump of a Norway rat and an Asia Minor gerbil also has this cadence[6].

Prediction 3. We next predict the occurrence of half-integer wave numbers in myriapod gaits. Because the network has twice as many cells as the animal has legs, the number of waves of leg movement that fit into the observable half of the network is either an integer or half an odd integer. Manton[25] provides drawings of several centipede gaits; the number of waves is close either to an integer (4, 3, 2) or half an odd integer (3/2); see Fig. 2. The tripod gait of hexapods[26] is a 3/2 wave.

Prediction 4. Finally, we specialize the network to bipeds where hidden cells seem unnecessary[9]. For evolutionary reasons, we expect bipeds not to break the pattern hypothesized for many-legged animals, thus resulting in four primary bipedal gaits (Table 2). If hidden cells do occur in bipedal CPGs, they should play an active role, perhaps controlling the timing of different muscle groups. Thus, muscle groups may reveal the presence of two distinct gaits in which the legs move half a period out of phase. More precisely, lower leg muscles should be activated synchronously in one gait and asynchronously in the other—because of the phases of the hidden cells. The human gaits walk and run support this prediction[27,28]. During walking, the gastrocnemius (an ankle plantarflexor) and the tibialis anterior (an ankle dorsiflexor) are activated out of phase, whereas during running, they are co-activated during significant portions of the gait cycle.

Unlike bipeds, the hidden phases of quadrupedal primary gaits can be deduced from the observable half network. Thus, each primary gait corresponds either to synchronous muscle activation (as in the run) asynchronous activation (as in the walk). This prediction should be testable. □

Received 21 May; accepted 9 August 1999.

1. Delcomyn, F. Neural basis of rhythmic behavior in animals. *Science* **210,** 492–498 (1980).
2. Grillner, S. Locomotion in vertebrates: central mechanisms and reflex interaction. *Physiol. Rev.* **55,** 247–304 (1975).
3. Selverston, A. I. Are central pattern generators understandable? *Behav. Brain Sci.* **3,** 535–571 (1980).
4. Shik, M. L. & Orlovsky, G. N. Neurophysiology of locomotor automatism. *Physiol. Rev.* **56,** 465–501 (1976).
5. Alexander, R. McN. in *Mechanics and Energetics of Animal Locomotion* (eds Alexander, R. McN. & Goldspink, J. M.) 168–203 (Chapman and Hall, London, 1977).
6. Gambaryan, P. P. *How Mammals Run: Anatomical Adaptations* (Wiley, New York, 1974).
7. Hildebrand, M. Symmetrical gaits of horses. *Science* **150,** 701–708 (1965).
8. Hildebrand, M. The quadrupedal gaits of vertebrates. *Bioscience* **39** (11) 766–775 (1989).
9. Collins, J. J. & Stewart, I. Coupled nonlinear oscillators and the symmetries of animal gaits. *J. Nonlin. Sci.* **3,** 349–392 (1993).
10. Golubitsky, M., Stewart, I., Buono, P. L. & Collins, J. J. A modular network for legged locomotion. *Physica D* **115,** 56–72 (1998).
11. Schöner, G., Jiang, W. Y. & Kelso, J. A. S. A synergetic theory of quadrupedal gaits and gait transitions. *J. Theor. Biol.* **142,** 359–391 (1990).
12. Collins, J. J. & Stewart, I. Symmetry-breaking bifurcation: a possible mechanism for 2:1 frequency-locking in animal locomotion. *J. Math. Biol.* **30,** 827–838 (1992).
13. Collins, J. J. & Stewart, I. Hexapodal gaits and coupled nonlinear oscillator models. *Biol. Cybern.* **68,** 287–298 (1993).
14. Collins, J. J. & Stewart, I. A group-theoretic approach to rings of coupled biological oscillators. *Biol. Cybern.* **71,** 95–103 (1994).
15. Kopell, N. & Ermentrout, G. B. Symmetry and phaselocking in chains of weakly coupled oscillators. *Comm. Pure Appl. Math.* **39,** 623–660 (1986).
16. Kopell, N. & Ermentrout, G. B. Coupled oscillators and the design of central pattern generators. *Math. Biosci.* **89,** 14–23 (1988).
17. Kopell, N. & Ermentrout, G. B. Phase transitions and other phenomena in chains of oscillators. *SIAM J. Appl. Math.* **50,** 1014–1052 (1990).
18. Buono, P.-L. & Golubitsky, M. Models of central pattern generators for quadruped locomotion: I. primary gaits. *J. Math. Biol.* (submitted).
19. Golubitsky, M., Stewart, I. N. & Schaeffer, D. G. *Singularities and Groups in Bifurcation Theory* Vol. 2 275–282 387–399 (Springer, New York, 1988).
20. Buono, P.-L. *A Model of Central Pattern Generators for Quadruped Locomotion.* PhD Thesis, Mathematics Department, Univer. Houston (1998).
21. Hildebrand, M. in *Neural Control of Locomotion* (eds Herman, R. M., Grillner, S., Stein, P. S. G. & Stewart, D. G.) 203–236 (Plenum, New York, 1976).
22. Alexander, R. McN. & Jayes, A. S. A dynamic similarity hypothesis for the gaits of quadrupedal mammals. *J. Zool.* **201,** 135–152 (1983).
23. Leach, D. H. & Sprigings, E. Gait fatigue in the racing thoroughbred. *J. Equine Med. Surg.* **3,** 436–443 (1979).
24. Deuel, N. R. & Lawrence, L. M. Laterality in the gallop gait of horses. *J. Biomech.* **20,** 645–649 (1987).
25. Manton, S. M. The evolution of arthropodan locomotory mechanics. Part 8: Functional requirements and body design in Chilopoda. *J. Linnaean Soc. (Zool.)* **45,** 251–484 (1965).
26. Full, R. J., Blickhan, R. & Ting, L. H. Leg design in hexapedal runners. *J. Exp. Biol.* **158,** 369–390 (1991).
27. Mann, R. A. in *Disorders of the Foot* (ed. Jahss, M. H.) 37–67 (W. B. Saunders, Philadelphia, 1982).
28. Mann, R. A., Moran, G. T. & Dougherty, S. E. Comparative electromyography of the lower extremity in jogging, running and sprinting. *Am. J. Sports Med.* **14,** 501–510 (1986).

Probing the human stereoscopic system with reverse correlation

Peter Neri, Andrew J. Parker & Colin Blakemore

University Laboratory of Physiology, Parks Road, Oxford OX1 3PT, UK

Our two eyes obtain slightly different views of the world. The resulting differences in the two retinal images, called binocular disparities, provide us with a stereoscopic sense of depth[1]. The primary visual cortex (V1) contains neurons that are selective for the disparity[2–4] of individual elements in an image, but this information must be further analysed to complete the stereoscopic process[5,6]. Here we apply the psychophysical technique of reverse correlation[7] to investigate disparity processing in human vision. Observers viewed binocular random-dot patterns, with 'signal' dots in a specific depth plane plus 'noise' dots with randomly assigned disparities. By examining the correlation between the observers' ability to detect the plane and the particular sample of 'noise' disparities presented on each trial, we revealed detection 'filters', whose disparity selectivity was remarkably similar to that of individual neurons in monkey V1. Moreover, if the noise dots were of opposite contrast in the two eyes, the